

Plasma dynamic synthesis of iron oxides in a discharge plasma jet with possibility to control final phase composition

I Shanenkov, A Sivkov, A Ivashutenko and M Gukov

Institute of Power Engineering, Tomsk Polytechnic University, Lenin av. 30, Tomsk, Russian Federation

E-mail: Swordi@list.ru

Abstract. Magnetite Fe_3O_4 and epsilon iron oxide $\epsilon\text{-Fe}_2\text{O}_3$, having excellent frequency characteristics and high electrical resistivity, are considered as the most promising phases among all iron oxides for high-frequency equipment in order to increase the working frequency of the data transmission. Despite the large number of existing methods for synthesizing these materials, many of them do not provide both of these phases. In opposite to these methods, the plasma dynamic synthesis can provide the synthesis of necessary phases in a one-step process. The process is implemented in an electrodischarge iron-containing plasma jet, which interacts with gaseous precursor (oxygen). The use of plasma jet allows obtaining nanoscale powdered products. This work shows the results of the experiment series, where the influence of initial energy parameters on the final phase composition was studied. It is found that the plasma dynamic synthesis allows obtaining both magnetite Fe_3O_4 and epsilon phase $\epsilon\text{-Fe}_2\text{O}_3$ during one short-term process (less than 1 ms). It is also established that the final phase composition strongly depends on the initial parameters of the system. The increased energy parameters lead to the formation of the product with predominant content of epsilon phase, while lower parameters allow synthesizing magnetite phase. Thus, by changing energy parameters, it is possible to control the final composition in the considered system.

1. Introduction

Magnetic iron oxides are of a great interest in research and industry. They have numerous applications in different areas, ranging from engineering (e.g., magnetic recording media or magnetic seals) to biomedical applications (e.g., magnetic resonance imaging, drug delivery or hyperthermia) and their appealing novel properties [1–5]. Among various magnetic iron oxides, those that exhibit soft magnetic behavior with excellent frequency characteristics and high electrical resistivity are strongly required as core materials used in magnetic components for the ceaseless increase of the working frequency of the data transmission and multiple accesses in computer, mobile and blue-tooth devices [6,7]. The most known iron oxide phases, having outstanding characteristics of electromagnetic radiation (EMR) absorption, are magnetite Fe_3O_4 and relatively new epsilon phase $\epsilon\text{-Fe}_2\text{O}_3$.

In the case of magnetite, the best EMR absorption properties are shown by hollow spheres of Fe_3O_4 [8,9]. They can provide a strong attenuation (up to –40 dB) of electromagnetic (EM) signal in a wide range of frequencies (from 2 to 18 GHz). Moreover, the hollow structure of these spheres allows obtaining low-weight coatings and samples, which protect from EMR. Absorbing materials based on epsilon phase can effectively attenuate the EM signal in a range of frequencies from 110 to 183 GHz,



which makes them very prospective for using in military applications. The main problem is the difficulties with its synthesis. It is known that this phase is thermally unstable (converts to hematite at temperatures about 750 °C) and can exist only in nanodispersed state (also converts to hematite when interacts with other particles due to low surface energy) [10].

In the past decades, preparations of magnetic iron oxide nanoparticles have been extensively studied, especially in synthesis chemistry. One has witnessed various methods (e.g., solid state reactions [11]; high energy ball milling [12]; sol-gel [13]; chemical co-precipitation [14]; conventional two-step synthesis [15], and so on) that have yielded various kinds of magnetic iron oxide nanoparticles. Nonetheless, not all of these methods allow synthesizing both ϵ -Fe₂O₃ and Fe₃O₄ phases and those which do suffer from such disadvantages as the process duration (usually, it is multi-step process, which can continue up to 24 hours or more), the necessity to use a large amount of expensive precursors and the low yield of the final product [16]. Differing from the preparation methods mentioned above, an alternative approach—plasma dynamic synthesis [17-19]—can provide synthesis of necessary phases in one-step process.

The aim of this work is to synthesize the soft magnetic phases of iron oxide by implementing the process in a discharge plasma jet using a coaxial magnetoplasma accelerator (CMPA). It is shown that the plasma dynamic method allows obtaining ultradispersed powders of iron oxide including both ϵ -Fe₂O₃ and Fe₃O₄ phases. It is found that the system energy parameters directly influence the ratio between these phases in the final product. It is suggested that the rate of current rise plays the key role in obtaining the powder with high content of epsilon phase by plasma dynamic method.

2. Experimental

Both the design and the function of CMPA-based system can be explained using Figure 1. In order to synthesize iron oxide powders, the system based on iron electrodes (central electrode 1 and barrel-electrode 6) was used. Electrodes were separated by a fiberglass insulator 2. All this assembly was held by metal cases 3 and placed into solenoid 5. Before starting the process, the capacitive energy storage C was charged. In the first moment of time (t_0), when the power keys 7 were closed, the energy from capacitive storage was released and the process was started. Current flow through electrodes and explosive Fe wires 4. When its value became large enough, Fe wires exploded forming the arc discharged plasma structure. This plasma structure was accelerated by forces of conductive and inductive electrodynamics. Iron, which was necessary for synthesis, was accumulated from the central electrode and inner walls of electrode-barrel due to their electro erosion. The gas precursor (O₂) was added into the working chamber, which was preliminary evacuated, through the gas collector.

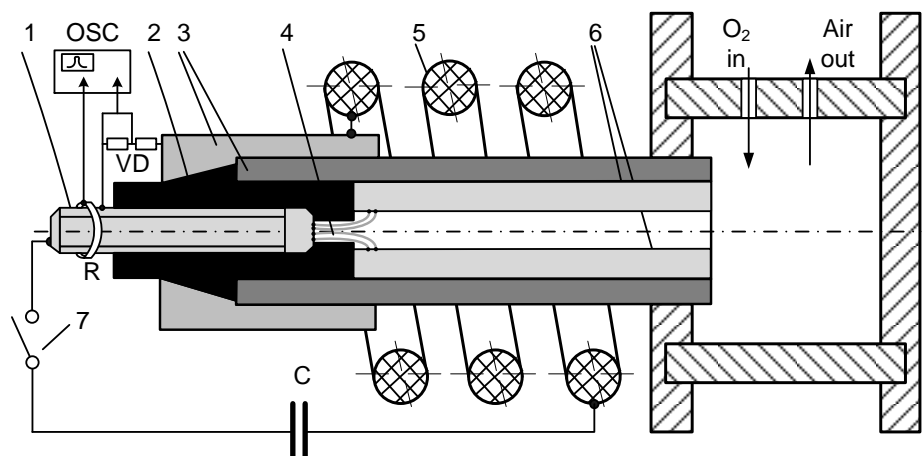


Figure 1. Sketch-map of the system.

During the process, such energy parameters as the discharge current and voltage between electrodes were recorded using Rogowski coil R and ohmic voltage divider VD , respectively. Both signals were recorded by Tektronix 2012b oscilloscope. Based on the current and voltage data, the discharge power and input energy were calculated.

A series of experiments was carried out in order to investigate the possibility to control the phase composition in the resulting powders by changing energy parameters of the system. The main data of experiments are shown in Table 1. It is worth noting that experiment 3 was carried out using without using Fe explosive wires. In order to initiate the discharge, carbon spray was used to create a thin conductive layer on the surface of the insulator's inner surface.

Synthesized powders were investigated using such methods as X-Ray diffractometry (XRD) and scanning electron microscopy (SEM). The XRD analysis was carried out using Shimadzu XRD7000S diffractometer with Shimadzu CM-3121 counter monochromator. In order to provide qualitative and quantitative analyses of XRD patterns, PowderCell 2.4 software and PDF2+ database were used. SEM analysis was carried out using Hitachi TM3000 microscope.

Table 1. Initial energy parameters of experiments and mass of products.

	Experiment 1	Experiment 2	Experiment 3
Charging voltage U_c [kV]	3.22	2.50	2.50
Charging capacity C_c [mF]	14.4	14.4	28.8
Charging energy W_c [kJ]	75.0	45.0	90.0
Input energy W [kJ]	57.8	24.2	67.2
W/W_c [%]	77.1	56.3	74.6
Eroded mass m_e [g]	9.0	2.5	7.1
Product mass m_{prod} [g]	7.3	2.0	6.6

3. Results and Discussions

As a result of each experiment, oscillograms of the voltage $v(t)$, current $i(t)$, power $p(t)$ and energy $w(t)$ were recorded (Figure 2). As it can be seen from oscillograms of current, the process had an aperiodic nature in all experiments. Such process feature can be explained by increasing the system's active resistance since a certain time moment. This leads both to an increase in the ratio between active resistance and inductive resistance, which in this system is practically unchanged, and to the transition to the aperiodic discharge. The main difference between experiments with Fe explosive wires and carbon spray was in the character of plasma structure formation. In the case with Fe wires, which had the resistance of few mOhm, in the first moment of time, after closing power keys, there was an immediate rise of current. It led to the explosion of Fe wires with the formation of plasma structure. In the case of carbon spray, there was a step of about 25 μ s, when the capacitive energy storage discharged on the high active resistance (~ 5 kOhm) of the thin layer. An aperiodic nature was also seen for this discharge. When the carbon layer was heated enough under the influence of current (~ 10 kA), the arc discharge started to burn, and the process was similar to experiments with Fe wires.

As can be seen from Table 1, the initially selected energy parameters significantly influenced the energy characteristics of the process. For example, at the minimum charging energy (experiment 2) the magnitude of the main parameters was lower than in other experiments. The maximum current value was equal to 113 kA, and the magnitude of the input energy was 24.2 kJ, while the efficiency of its conversion was 56%. The higher initial energy parameters (experiments 1 and 3), the higher the maximum current (up to ~ 225 kA) and the energy conversion efficiency ($\sim 75\%$). The increase in current led to an increase in the mass of eroded material and in the mass of the final product.

The formation process of ultra- and nanodispersed particles in the CMPA-based system was considered in detail earlier [20]. The higher current leads to the increase in the temperature and plasma flow speed. In turn, this influences the increase in the temperature gradient and the speed of

the material sputtering from the front of the bow shock wave in the chamber-reactor. Both of these factors have a significant effect on the cooling rate and the final dispersivity of the material. It is known that the epsilon phase $\epsilon\text{-Fe}_2\text{O}_3$ can exist only when its particle sizes are less than 200 nm. Thus, the increase in the energy parameters of the experiment and, in particular, the increase in the current level have to directly impact the phase composition of the final synthesized samples.

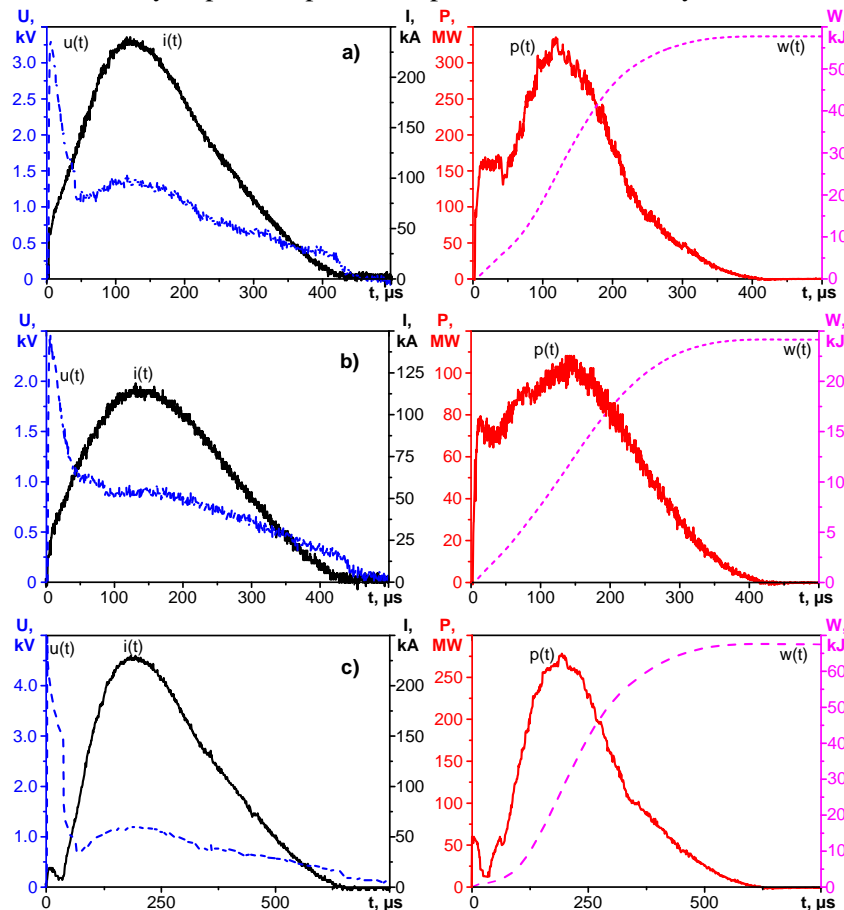


Figure 2. Oscillograms of current $i(t)$, voltage $u(t)$, discharge power $p(t)$ and input energy $w(t)$, recorded during implementing the experiments: a) exp. 1; b) exp. 2; c) exp. 3.

All synthesized samples were studied using X-Ray diffractometry (XRD) method. XRD patterns of products are shown in Figure 3. Table 2 contains the results of the quantitative analysis of phase composition carried out using a PowderCell 2.4 software and PDF2+ database, together with the additional data obtained after a more detailed study of oscillograms (pulse time, max current, max voltage and current rising edge). The comparison of XRD patterns shows that in the experiment with low energy parameters (experiment 2), the peaks corresponding to hematite and epsilon phases are low-intensity and present in the form of traces. In turn, magnetite peaks have the greatest intensity and are more clearly seen in comparison with XRD patterns for products of other experiments. As for the other two experiments with high energy parameters, they are characterized by the presence of well-seen maxima of epsilon and hematite phases. The presence of hematite in the final product is quite likely due to the fact that the synthesized nanoparticles $\epsilon\text{-Fe}_2\text{O}_3$ have a low surface energy, and in the process of sputtering from the front of the bow shock wave they can interact with each other. This, ultimately, leads to their growth and transition to the $\alpha\text{-Fe}_2\text{O}_3$ phase.

A more detailed analysis of oscillograms allowed establishing the relationship between the level of the current, the front of its rising and the final phase composition (Table 2). It was found that the higher level of discharge current influence the yield of the epsilon phase in the final product. Such

feature seems to be natural due to the fact that the larger value of the discharge current causes a greater temperature gradient, which, in turn, leads to an increase in the cooling rate and the formation of smaller particles. Because ϵ -Fe₂O₃ can exist only, when its particles less than 200 nm, the obtaining of higher energy parameters is necessary condition for the considered system to obtain the product with higher yield of ϵ -Fe₂O₃ phase. In fact, when the maximum current value is equal to 113.0 kA (exp. 2), the ϵ -Fe₂O₃ content is 13.0%. With increase in current level up to ~225 kA, the content of epsilon phase is also increased up to 37.0% (exp. 1) and 50.0% (exp. 3).

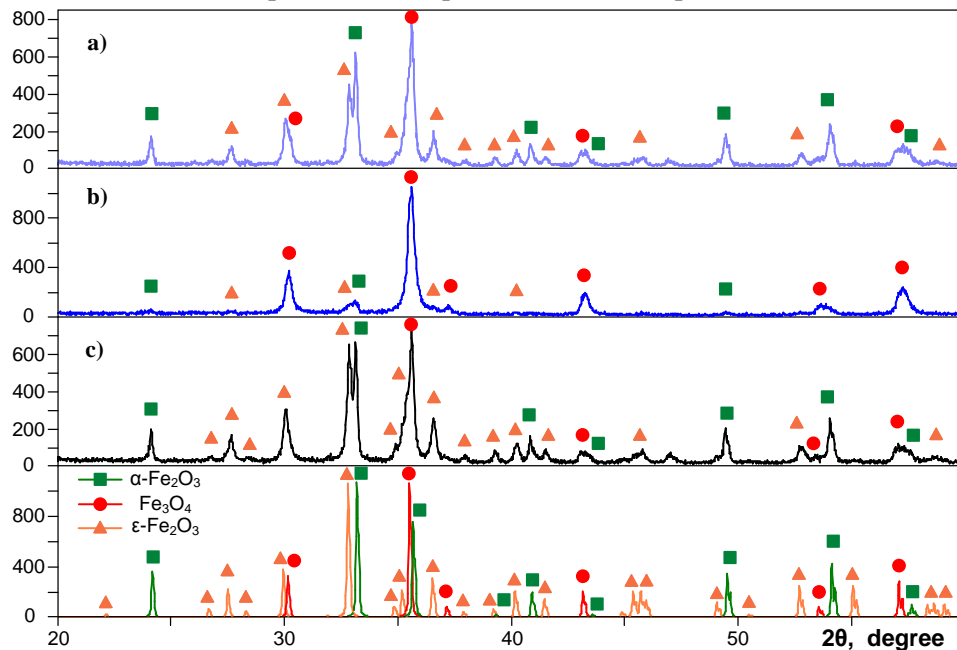


Figure 3. XRD patterns of the products synthesized in different experiments: a) 1; b) 2; c – 3); as well as reference models of iron oxide phases from PDF2+ database.

Table 2. Energy parameters of experiments and phase composition of products

		Experiment 1	Experiment 2	Experiment 3
Energy parameters	Charging voltage U_c [kV]	3.22	2.45	2.50
	Charging capacity C_c [mF]	14.4	14.4	28.8
	Pulse time t_p [μs]	405.0	415.0	610.0
	Max current I_m [kA]	231.0	113.0	225.5
	Max voltage U_m [kV]	1.39	0.94	1.21
	Input energy W [kJ]	57.8	24.2	67.2
	Rate of current rise di/dt [a.u.]	1.80	0.94	2.12
Phase composition	ϵ -Fe ₂ O ₃ [wt%]	36.7	13.0	50.0
	Fe ₃ O ₄ [wt%]	36.0	76.5	24.0
	α -Fe ₂ O ₃ [wt%]	27.3	10.5	26.0

In spite of being almost equal maximum discharge currents, experiments 1 and 3 differ from each other with the content of epsilon phase. This fact can be explained by the difference in the rate of the current rise. According to Table 2, this parameter is equal to 2.12 for experiment 3 and 1.80 for experiment 1. The rate of current rise shows the speed of energy input, which influences the speed of the plasma flow. In turn, the speed of plasma flow directly influences the speed of material sputtering, which is necessary for obtaining the nanoscale particles. Thus, when the rate of current rise is higher, the synthesized product has a less particle size that leads to formation of the powder with the predominant content of epsilon phase. In opposite to experiments with high energy parameters, the

experiment, where the maximum current is equal to 113.0 kA, showed the high yield of magnetite Fe_3O_4 . This seems to be natural due to the same reasons discussed above. When the current and its rise rate are decreased, there is a reduction of main plasma parameters that negatively influences the conditions for epsilon phase formation. In this case, magnetite becomes a dominant phase in the product. Thus, the CMPA-based system allows not only synthesizing soft magnetic phases of iron oxide but also controlling their ratio in the final product. This control is implemented by changing the initial energy parameters of the capacitive energy storage, which is used for power supplying the CMPA, and by changing the way of the plasma structure formation. Despite the found dependence on the maximum level of discharge current, there is a limit value for energy parameters, which cannot be exceeded, in order to provide the reliable work of the system.

4. Conclusion

Soft magnetic phases of iron oxide (magnetite Fe_3O_4 and epsilon $\epsilon\text{-Fe}_2\text{O}_3$) can be synthesized in one-step short-term (less than 1 ms) process using the plasma dynamic method in the system based on the coaxial magneto plasma accelerator. The synthesis is implemented in an electric-discharge iron-containing plasma jet flowing into oxygen atmosphere. It is found that the energy parameters of the process sufficiently influence the phase composition of the final product. The content of epsilon phase strongly depends on the level of discharge current and rate of its rising. The higher these parameters can be reached, the more yield of the epsilon phase can be obtained. In opposite, at lower energy parameters Fe_3O_4 phase dominates in the final product. Thus, the CMPA-based system allows controlling the final phase composition by changing the energy parameters.

References

- [1] Majetich S and Sachan M 2006 *J. Phys. D: Appl. Phys.* **39** R407
- [2] Leslie-Pelecky D L and Rieke R D 1996 *Chem. Mater.* **8** 1770
- [3] Frey N A, Peng S, Cheng K and Sun S 2009 *Chem. Soc. Rev.* **38** 2532
- [4] Lu A H, Salabas E L and Schuth F 2007 *Angew. Chemie - Int. Ed.* **46** 1222
- [5] Estrader M, Roca a G and Nogués J 2015 *Phys. Rep.* **553** 1
- [6] Pardavi-Horvath M 2000 *J. Magn. Magn. Mater.* **215** 171
- [7] Toneguzzo P, Viau G, Acher O, Fiévet-Vincent F and Fiévet F 1998 *Adv. Mater.* **10** 1032
- [8] Wei J, Liu J and Li S 2007 *J. Magn. Magn. Mater.* **312** 414
- [9] Liu Y, Cui T, Li Y, Zhao Y, Ye Y, Wu W and Tong G 2016 *Mater. Chem. Phys.* **173** 152
- [10] Tucek J, Zboril R, Namai A and Ohkoshi S I 2010 *Chem. Mater.* **22** 6483
- [11] Lu J, Yang S, Ng K M, Su C-H, Yeh C-S, Wu Y-N and Shieh D-B 2007 *Nanotechnology* **18** 289001
- [12] Munoz J E, Cervantes J, Esparza R and Rosas G 2007 *J. Nanoparticle Res.* **9** 945
- [13] da Costa G M, De Grave E, de Bakker P M a. and Vandenberghe R E 1994 *J. Solid State Chem.* **113** 405
- [14] Khalil M I 2015 *Arab. J. Chem.* **8** 279
- [15] Lind K, Kresse M, Debus N P and Müller R H 2002 *J. Drug Target.* **10** 221
- [16] Syue M R, Wei F J, Chou C S and Fu C M 2011 *J. Appl. Phys.* **109** 101
- [17] Sivkov A A, Ivashutenko A S, Nazarenko O B, Saigash A S, Pak A Y and Kolganova Y L 2016 *Inorg. Mater. Appl. Res.* **7** 354
- [18] Shanenkov I I, Sivkov A A, Pak A Y and Kolganova Y L 2014 *Adv. Mater. Res.* **1040** 813
- [19] Kuzenov V V, Polozova T N and Ryzhkov S V 2015 *Problems of Atomic Science and Technology* **4 (98)** 49.
- [20] Sivkov A, Naiden E, Ivashutenko A and Shanenkov I 2016 *J. Magn. Magn. Mater.* **405** 158

Acknowledgements

This work was supported by the Russian Science Foundation (grant No. 15-19-00049).